Influence of octacalcium phosphate coating on osteoinductive properties of biomaterials

P. HABIBOVIC[1,2*], C. M. VAN DER VALK[2], C. A. VAN BLITTERSWIJK[1,2], K. DE GROOT[1,2]
[1]*Institute of Biomedical Technology, Twente University, Department Bilthoven, Professor Bronkhorstlaan 10-D, 3723 MB, Bilthoven, The Netherlands*
[2]*IsoTis SA, Bilthoven, The Netherlands*
E-mail: Pamela.habibovic@isotis.com

G. MEIJER[3]
[3]*University Medical Center Utrecht, The Netherlands*

In this study, we investigated the influence of octacalcium phosphate (OCP) coating on osteoinductive behaviour of the biomaterials.

Porous titanium alloy (Ti6Al4V), hydroxyapatite (HA), biphasic calcium phosphate (BCP) and polyethylene glyco terephtalate/polybuthylene terephtalate (PEGT–PBT) copolymer, all uncoated and coated with biomimetically produced OCP, were implanted in back muscles of 10 goats for 6 and 12 weeks. Uncoated Ti6Al4V and HA did not show any bone formation after intramuscular implantation. All OCP coated implants, except PEGT–PBT, did induce bone in the soft tissue. The reason for the non-inductive behaviour of the copolymer is probably its softness, that makes it impossible to maintain its porous shape after implantation. Both uncoated and OCP coated BCP induced bone. However, the amount of animals in which the bone was induced was higher in the coated BCP implants in comparison to the uncoated ones.

Osteoinductive potential of biomaterials is influenced by various material characteristics, such as chemical composition, crystallinity, macro- and microstructure.

OCP coating has a positive effect on osteoinductivity of the biomaterials. The combination of the advantages of biomimetic coating method above traditional methods, and a good osteoinductivity of OCP coating that is produced by using this method, opens new possibilities for designing more advanced orthopaedic implants.

1. Introduction

Osteoinduction can be defined as the process of bone formation in extraskeletal sites. Osteoinduction includes a process of differentiation of non-osteogenic cells into osteoblasts and bone morphogenesis.

Various calcium phosphate (CaP) containing biomaterials, produced in the form of ceramics, cements and coatings, have been shown to induce ectopic bone formation in various animal models. In the last decade, a few cases of bone induction were reported by synthetic hydroxyapatite (HA) in dogs [1–5], coral-derived HA in dogs, monkeys and baboons [5–7], synthetic alpha- and beta-tricalcium phosphate (α-TCP, β-TCP), biphasic calcium phosphate ceramics (BCP), α-pyrophosphate ceramics and β-pyrophosphate ceramics [8–13]. Besides many reports of osteoinduction by CaP ceramics, Yuan *et al.* [14] showed ectopic bone formation by a CaP cement in muscles of dogs. Recently, Yuan *et al.* and Barrere *et al.* [15, 16] reported osteoinduction by octacalcium phosphate (OCP) coating on porous tantalum (Ta) implants in dogs and goats, respectively.

CaP coatings on metal implants are one of the examples of combining different biomaterials in order to design a better orthopaedic implant. Combination of sufficient mechanical properties of metals with bioactivity of CaPs makes CaP coated implants suitable for, for example, total hip arthroplasty and other load bearing applications. The conventional technique of providing metal implants with a CaP coating is plasma-spraying (PS). Although PS coated implants have shown great clinical successes [17], the method of producing these coatings shows many disadvantages. This kind of process is taking place at very high temperatures, limiting PS method to stable CaP phases. Furthermore, it is not possible to coat geometrically complex and porous implants by using this method. On the other hand, introduction of porosity into orthopaedic implants is becoming more important, as mechanical interlocking might enhance the bone–implant integration process.

Recently, other techniques have been studied to improve the quality of coatings, such as electrophoretic deposition [18], sputter deposition [19] and sol–gel [20].

*Author to whom all correspondence should be addressed.

Nevertheless, the deposition of CaP coatings from simulated body fluids (SBF) [21] offers the most promising alternative to PS and other methods. The biomimetic coating method is inspired by the bone mineralisation process of collagen fibers. As a result of the paraphysiological conditions of this technique, various CaP phases such as OCP [22] and carbonated apatite (CA) [23] can be deposited. This process is taking place in a solution, making it possible to coat geometrically irregular and porous implants.

Study by Barrere *et al*. [16] showed that on porous Ta implants, biomimetic OCP coating was able to induce bone in the muscles of goats, while no bone was found in CA coated implants. Furthermore, bone was solely induced inside the pores and never on the flat implant surfaces.

The objective of this study was to study influence of biomimetic OCP coating on osteoinductive properties of various biomaterials in goats.

2. Materials and methods

2.1. Implants

In this study, we used four kinds of porous materials: Ti6Al4V, HA, BCP and PEGT–PBT. All materials, except PEGT–PBT were used with and without biomimetic OCP coating.

Ti6Al4V implants were produced by a positive replica method as described earlier [24]. In short, 70 wt % of titanium alloy powder (Northwest Non-Ferrous Institute of China) consisting of spherical particles with a diameter lower than 44 μm (325 mesh) was mixed with H_2O (20 wt %). Polyethylene glycol (PEG) and methyl-cellulose were used as binders (8 wt %). Dolapix (CE 64, Germany) and ammonia solution (2 wt %) were added to improve the rheological property of the slurry. Porous titanium alloy bodies were made by impregnation of polymeric (PU) sponges (35–45 pores per inch) (Coligen Europe BV, Breda, The Netherlands). When the slurry reached the designed viscosity range (3000–5000 cp), polyurethane (PU) foams were dipped into the slurry and then extracted to dry. The dipping–drying process was repeated until the struts of the PU foam were coated with titanium alloy slurry. The superfluous slurry was removed by using a roller under pressure, to get an evenly distributed coating on the foam. After final drying, the samples were first heated to 500 °C to burn out foam, then they were sintered in a vacuum furnace at 1250 °C with holding time of 2 h. Cylinders ($\varnothing 5 \times 10\,mm^2$) were machined by using the electric sparkling method. The ultrastructure of porous titanium alloy was characterised by using an environmental scanning electron microscope (ESEM; XL30, ESEM-FEG, Philips, The Netherlands). The porosity of the material was determined from the histological slides using an image analysis PC-based system equipped with KS400 version 3.0 software (Carl Zeiss Vision, Oberkochen, Germany). Average pore size was measured on the 2-D cross-sections by using the automatic ruler of the ESEM. Pore interconnectivity was visually analysed by the ESEM on the material cross-sections.

Porous HA implants were produced by using the dual phase mixing method described earlier [12]. In this method, commercially available HA powder (Merck, Amsterdam, The Netherlands) was used. The processing route consisted of three steps. In the first step, HA slurry was prepared by mixing 2/3 wt % of calcined HA powder with 1/3 wt % water containing deflocculant (Dolapix CE 64, Germany) and binder (carboxyl-methyl cellulose, Pomosin BC, The Netherlands). In the second step, two immiscible phases were mixed: water-based HA slurry and polymethyl methacrylate (PMMA) resin with a volume ratio of 1 : 1. The PMMA resin consisted of PMMA powder, MMA monomer and an additional fugitive pore maker (< 10 v/v %) such as naphthalene or wax particles. In the final step, the mixture was mould-shaped, polymerised, dried, pyrolised and sintered in air at 1250 °C for 8 h. Cylinders ($\varnothing 5 \times 10\,mm^2$) were machined into cylinders ($\varnothing 5 \times 10\,mm^2$) using a lathe. The structure of porous HA was characterised by ESEM. Porosity, pore size and pore interconnectivity were analysed by the same techniques as described for the Ti6Al4V implants. Composition and crystal structure of the material were determined by using Fourier transform infra red spectroscopy (FTIR; Spectrum100, Perkin Elmer Analytical Instruments, Norwalk, CT) and X-ray diffraction (XRD; Miniflex, Rigaku, Japan).

Porous BCP implants were prepared by using the so-called H_2O_2 method as published earlier [12]. For the preparation of the ceramic, in-house made BCP powder was used. Porous green bodies were produced by mixing this powder with 2% H_2O_2 solution (1.0 g powder/ 1.2 ± 0.05 ml solution) and naphthalene (Fluka Chemie, The Netherlands) particles (710–1400 μm; 100 g powder/ 30 g particles) at 60 °C. The naphthalene was then evaporated at 80 °C and the green porous bodies were dried. Finally, the bodies were sintered at 1200 °C for 8 h. These bodies were machined into cylinders ($\varnothing 5 \times 10\,mm^2$) using a lathe. The structure of porous BCP was characterised by ESEM. Porosity, pore size and pore interconnectivity were analysed by the same techniques as described for the Ti6A14V implants. Composition and crystal structure were determined by using FTIR and XRD. HA/β-TCP weight ratio in the BCP was calculated by comparing the BCP XRD pattern to the calibration patterns prepared from the powders with the known HA/β-TCP weight ratios.

PEGT–PBT copolymers were obtained from IsoTis SA (Bilthoven, The Netherlands) with a composition denoted as *a*PEGT*b*PBT*c*, where *a* represents PEG molecular weight, and *b* and *c* wt % of PEGT and PBT blocks, respectively. Final materials were prepared by using the compression moulding and particle-leaching method described earlier [25]. In brief, PEGT–PBT granules with a size of 500–600 μm were homogeneously mixed with sodium chloride grains and sieved to obtain particles ranging in size of 400–600 μm. The amount of the salt was adjusted to a desired final volume percentage of 75%. The mixture was heated to 180 °C for 3 min and subsequently compression moulded for 1 min at 2.9 MPa in a hot press (THB 008, Fontijne Holland BV, The Netherlands) resulting in a block with dimensions of $120 \times 100 \times 10\,mm^3$. The block was then immersed into demineralised water for 48 h to remove the sodium chloride, and dried under reduced pressure in vacuum oven. Final implants with a size of $\varnothing 5 \times 10\,mm^2$ were

TABLE I Inorganic composition (mM) of Kokubo's SBF, supersaturated SBF × 5 and SCS

	Ion concentration (mM)							
	Na^+	K^+	Ca^{2+}	Mg^{2+}	Cl^-	HPO_4^{2-}	HCO_3^-	SO_4^{2-}
SBF	142.0	5.0	2.5	1.5	148.8	1.0	4.2	0.5
SBF × 5	714.8	—	12.5	7.5	723.8	5.0	21.0	—
SCS	140.4	—	3.1	—	142.9	1.86	—	—

cored out of bigger blocks. The structure of porous PEGT–PBT was characterised by ESEM. Porosity, pore size and pore interconnectivity were analysed by the same techniques as described for other implants.

2.2. Coating process

Prior to the coating process, porous implants were ultrasonically cleaned in acetone, ethanol and water, subsequently. Next, they were soaked in SBF for 24 h at 37 °C to seed the material surface with calcium phosphate nuclei. The used SBF solution was five times more concentrated than Kokubo's SBF solution [21] (Table I) in order to speed up the coating process. In order to produce crystalline OCP coating, the implants were then immersed in simulated calcifying solution (SCS) (Table I) for 48 h at 37 °C with one replenishment. The biomimetic method of producing the OCP coating has previously been described in detail [22]. The coating composition and crystallinity were investigated by using FTIR and XRD. Coating thickness was measured on 2-D implant cross-sections by the automatic ESEM ruler.

2.3. *In vivo* experiments

This study was approved by the Dutch Animal Care and Use Committee. Ten adult Dutch milk goats were used and housed at Central Animal Laboratory Institute (GDL), Utrecht, The Netherlands, at least four weeks prior to surgery.

Before the surgical procedure, a dose of 0.1 ml in 5 ml of physiologic saline solution (± 1 ml/25 kg body weight) of Domosedan (Pfizer Animal Health BV, Capelle a/d Ijssel, The Netherlands) was administered by intravenous injection. The surgical procedure itself was performed under general inhalation anaesthesia of the animals. Thiopental (Nesdonal, ± 400 mg/70 kg of body weight, on indication, Rhone Merieux, Amstelveen, The Netherlands) was injected intravenously, and anaesthesia was maintained with a gas mixture of nitrous oxide, oxygen and Halothane (ICI-Farma, Rotterdam, The Netherlands).

Besides the implantations described in this study, the animals were used for a different study, to be published separately. Based on the previous studies by our group, we hypothesize that different groups of implants could not influence each other's behaviour.

After shaving the lumbar area and disinfection with iodine, the left muscle fascia was exposed and cut. Using blunt dissection, intramuscular pockets were created, and filled with the above described implants: Ti6Al4V, OCP Ti6Al4V, HA, OCP HA, BCP, OCP BCP and OCP PEGT–PBT. Subsequently, the fascia was closed with a non-resorbabale suture to facilitate implant localisation at explantation. The skin was closed in two layers. After six weeks, the same procedure was repeated in the right back muscle. Table II gives an overview of the implanted materials.

Immediately after the surgery, pain relief was given by buprenofine (Temgesic; Schering-Plough, Kenilworth, NJ).

Twelve weeks after the first implantation (i.e. implantation times 6 and 12 weeks), each animal was sacrificed by an overdose of pentobarbital (Euthesaat, Organon, Oss, The Netherlands) and potassium chloride.

Intramuscular implants with surrounding tissue were explanted by sharp dissection and fixed in Karnovsky's fixative. All implants were dehydrated in a graded ethanol series (70–100%) and transferred into a MMA solution that polymerised at 37 °C within 1 week. Longitudinal sections (10–15 μm) were made by using the modified interlocked diamond saw (Leica Microtome, Nussloch, Germany). Sections were stained with 1% methylene blue and 0.3% basic Fuchsin after etching with HCl/ethanol mixture. Qualitative analysis was performed on all retrieved implants by using a light microscope (E600 Nikon, Japan).

3. Results

3.1. Implant characterisation

As determined from the material cross-sections by using the image analysis system, the average porosity of the porous Ti6Al4V implants was 79 ± 5% and the pore size varied between 400 and 1300 μm. Observations by the ESEM showed that the pores were well interconnected. Fig. 1(a) shows the structure of the uncoated porous Ti6Al4V. Higher magnification ESEM photograph (Fig. 1(b)) shows the rough metal surface, caused by the sintering of the alloy powder particles.

TABLE II Implantation scheme

	Material						
	Ti6Al4V	OCP Ti6Al4V	HA	OCP HA	BCP	OCP BCP	OCP PEGT–PBT
6 weeks	10	10	10	10	10	10	10
12 weeks	10	10	10	10	10	10	10

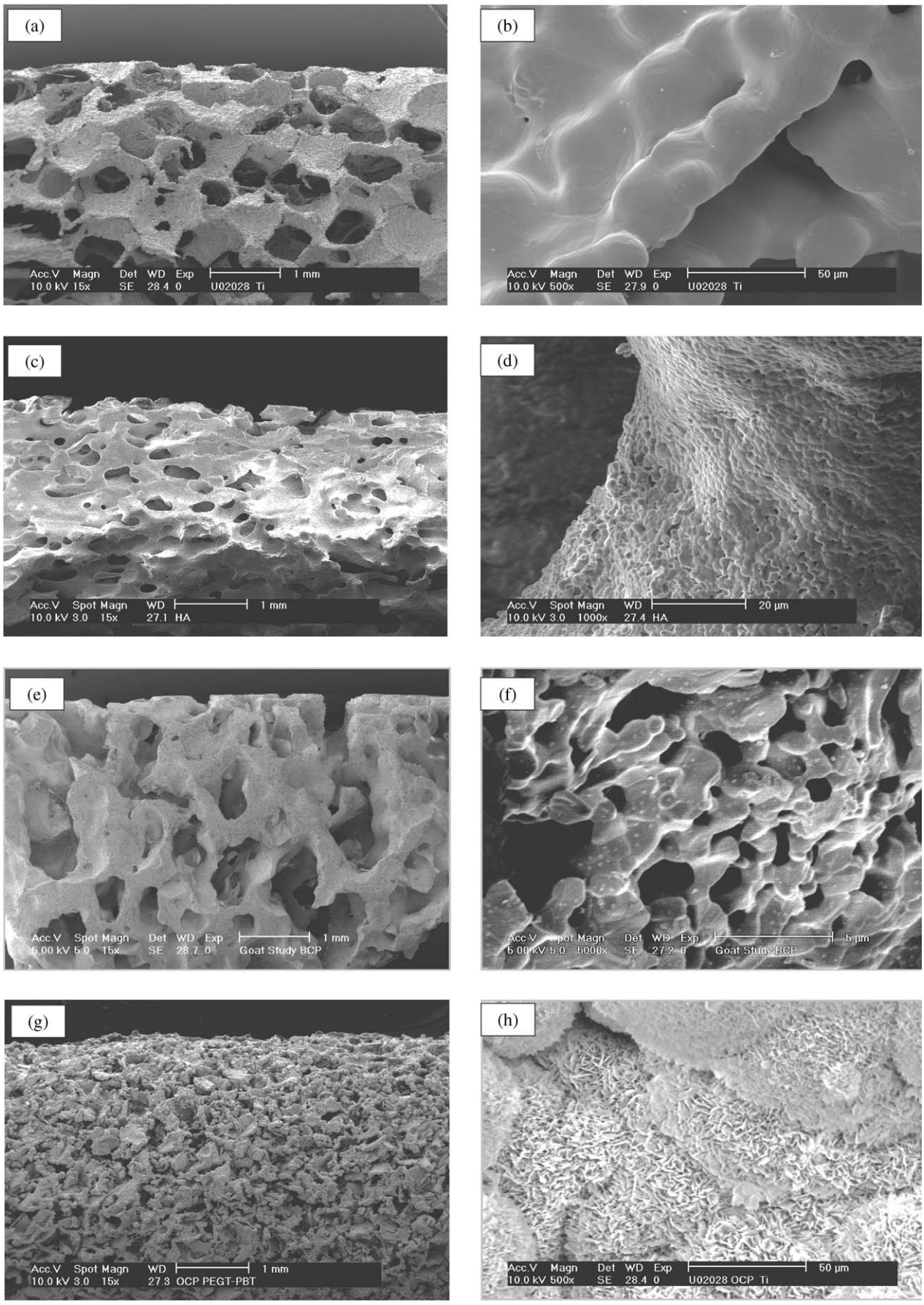

Figure 1 ESEM photographs of Ti6Al4V magnification 10 × (a), and 500 × (b), HA 10 × (c) and 1000 × (d), BCP 10 × (e) and 5000 × (f), OCP PEGT–PBT 10 × (g) and 500 × (h). High magnification OCP PEGT–PBT photograph is representative for the structure of OCP coating on all implants.

Average macroporosity of the porous HA implants was $46 \pm 8\%$ with pores varying in size between 100 and 800 µm. Mercury porosimeter measurements showed that the average microporosity ($< 10\,\mu m$) was around 1.3%. ESEM observations revealed that the pores were well interconnected. ESEM photograph at low magnifi-

cation (Fig. 1(c)) illustrates macroporous structure of HA, while the higher magnification photograph (Fig. 1(d)) shows its rough microstructure. XRD and FTIR analysis (results not shown) showed that the HA ceramic consisted of pure HA.

BCP implants showed a well-interconnected macroporous structure (Fig. 1(e)), with pores varying in size between 100 and 800 μm. Image analysis of the material cross-sections gave an average macroporosity of $54 \pm 4\%$. Higher magnification ESEM analysis (Fig. 1(f)) showed that macropore walls contained micropores (pore size $< 10\,\mu m$). As measured by mercury porosimeter, average microporosity was around 44%. XRD pattern and FTIR spectrum analyses (results not shown) of the produced material showed a biphasic chemistry consisting of 88% HA and 12% β-TCP. The material was highly crystalline.

Final composition of PEGT–PBT implants was 1000PEGT70PBT30, meaning the PEG molecular weight of 1000 and a weight percentage of PEGT/PBT being 70 and 30, respectively. The average porosity of these implants was $75 \pm 5\%$ and their pore size varied between 500 and 600 μm. Fig. 1(g) is a low magnification ESEM photograph of the OCP coated PEGT–PBT implant. High magnification photograph (Fig. 1(h)), that is representative for all kinds of OCP coated implants, shows the highly crystalline and rough structure of the final OCP coating.

ESEM observations revealed that in all coated implants, the material surface was homogeneously covered with a CaP layer. However, the thickness of the coating was not the same throughout the implant. The average thickness varied between 20 μm at the interior of the implant and 60 μm at the implant periphery. Large OCP crystals were oriented perpendicularly to the surface of the implants, as illustrated by the high magnification ESEM photograph of the coated PEGT–PBT (Fig. 1(h)). FTIR spectrum of the coating on the periphery of implants (spectra not shown) was typical for a pure, highly crystalline OCP phase. XRD pattern (not shown) of the OCP coating formed on a flat implant supported the FTIR findings.

3.2. Bone induction

At retrieval, all implants were surrounded by highly vascularised muscle tissue. Histology showed no evidence for toxicity of the implants nor was a deviating inflammatory reaction observed.

Table III shows bone incidence in all implants after 6 and 12 weeks of intramuscular implantation. As can be seen, uncoated Ti6Al4V and uncoated HA implants did not show any ectopic bone formation after 6 and 12 weeks of implantation. Bone could be observed in the uncoated BCP implants. All OCP coated implants, except PEGT–PBT, sporadically induced bone after both 6 and 12 weeks of intramuscular implantation. The amount of bone was limited in quantity.

TABLE III Bone incidence after intramuscular implantation

Material	6 weeks	12 weeks
Ti6Al4V	0/10	0/10
OCP-Ti6Al4V	4/10	6/10
HA	0/10	0/10
OCP-HA	2/10	0/10
BCP	3/10	6/10
OCP-BCP	4/10	6/10
OCP-PEGT–PBT	0/10	0/10

The macropores of all implants were filled with fibrous tissue. The bone formed in BCP, OCP Ti6Al4V, OCP HA and OCP BCP was always observed in the macropores inside the implants and never on the outer surface or in the surrounding soft tissue. The formed bone was normal in appearance, aligned with osteoblasts, and with mineralised bone matrix and osteocytes clearly visible. Fig. 2 shows light microscope photographs of all implants after 12 weeks of implantation. In Ti6Al4V, HA and OCP PEGT–PBT (Fig. 2(a), (c), and (g) respectively), we observed fibrous tissue filling the pores. Bone induction is illustrated in OCP Ti6Al4V, OCP HA, BCP and OCP BCP in LM photographs Fig. 2(b), (d), (e) and (f) respectively. Cartilage formation was not observed in any of the implants, indicating that the process of bone formation followed the intramembraneous ossification route.

The OCP coating was often incorporated into the newly formed bone. In the areas without bone, the OCP coating had extensively dissolved after 6 weeks, and could only occasionally be observed after 12 weeks of implantation. In the areas where the coating was still visible, signs of its resorption by multinucleated cells could be observed.

4. Discussion

In this goat study, we investigated the effect of OCP coating on osteoinductive potential of various biomaterials.

First of all it is interesting to note that large differences were observed in the amount of bone that was induced in individual animals, that is, one goat was ''more inductive'' than another goat, for all implanted materials. The reason for these differences could be searched in genetic as well as in pathological background, but as long as the mechanism of osteoinduction itself is not clear, this phenomenon will be hard to explain. Furthermore, from various studies on osteoinduction by CaPs it is well known that different kinds of animals also posses different ''osteoinductive potentials''. For instance, if we would implant the identical material in muscles of dogs and goats, more bone would be induced in the first case.

Because of the limited amount of goats in which bone was induced in this study, and a low quantity of the formed bone, we decided to only qualitatively analyse the ectopic bone formation.

All materials used in this study had a macroporous structure. The reason for this choice of structure was the fact that in all previous studies on osteoinduction by CaP biomaterials, ectopic bone formation was never observed on dense or on the peripheries of porous implants, suggesting that the existence of porosity is one of the prerequisites for osteoinduction.

Furthermore, this study showed that the uncoated

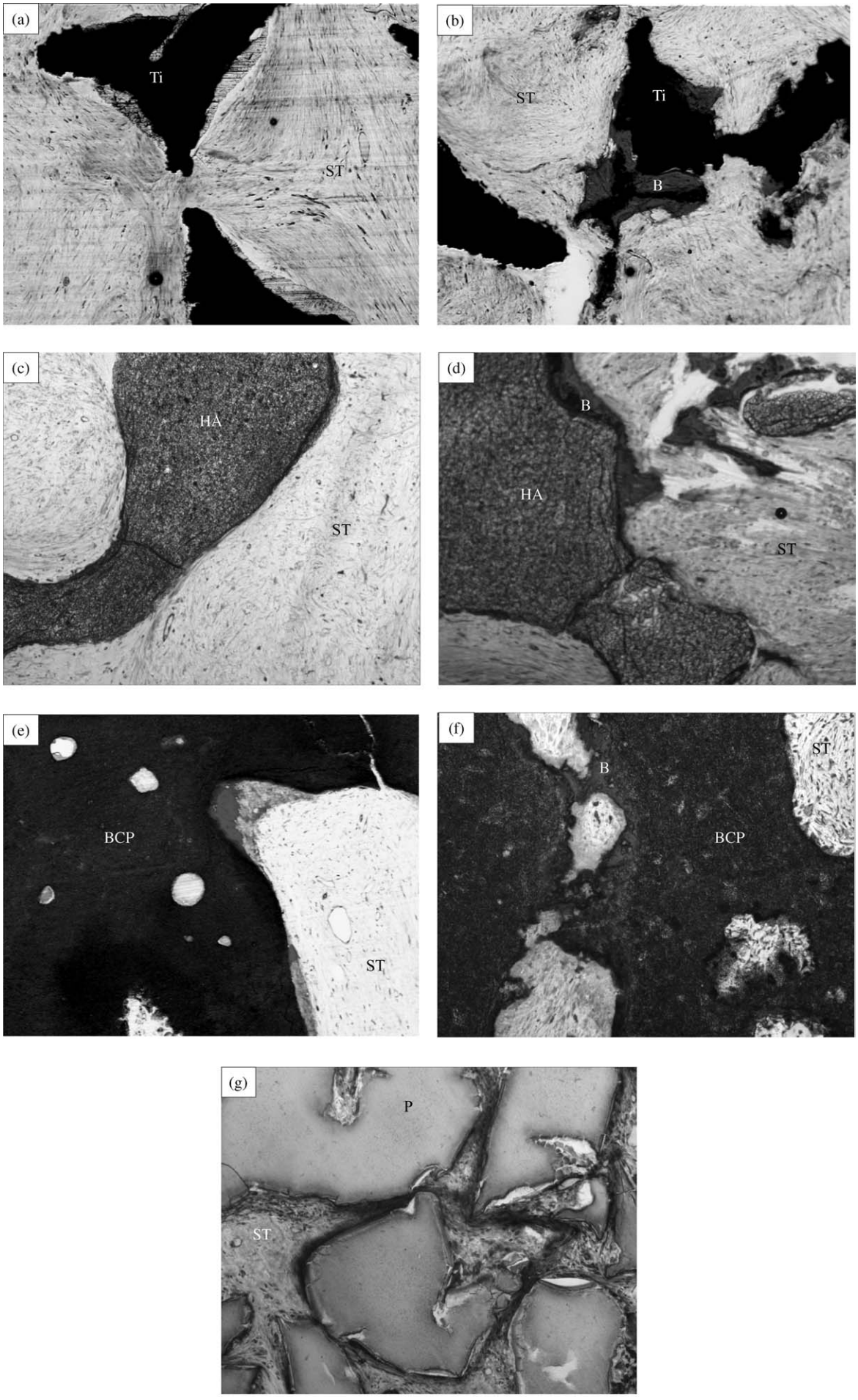

Figure 2 LM photographs (magnification 10 ×) after 12 weeks of intramuscular implantation of Ti6A14V (a), OCP Ti6Al4V (b), HA (c), OCP HA (d), BCP (e), OCP BCP (f) and OCP PEGT–PBT (h); Ti – titanium alloy, HA – hydroxyapatite, BCP – biphasic calcium phosphate, P – PEGT–PBT, ST – soft tissue and B – bone.

metal implant did not induce bone formation, but after application of the CaP coating on its surface, the bone was induced. This suggests that the presence of CaP on an implant is also a prerequisite for ectopic bone formation. Yuan *et al*. [26] and Fujibayashi *et al*. [27] showed the possibility of bone induction by alumina ceramic and chemically treated porous titanium respectively. However, both materials were shown to be able to easily calcify when immersed in SBF *in vitro*, suggesting that the same process of calcification is taking place *in vivo* as well, before the start of bone formation. This emphasises the importance of CaP in bone induction. However, only the presence of a CaP phase is not enough, as is suggested by the fact that no bone was found in uncoated HA implants. So we can conclude that a combination of the right CaP phase with the right implant geometry is the way of producing an osteoinductive orthopaedic implant.

The above described implant characterisation shows that in this study we compared different CaP phases (HA, BCP and OCP) as well as different macro- and microstructures. In the case of bulk ceramics, sintering process is often responsible for the formation of micropores inside the macropore walls. Therewith, the surface roughness of the ceramic is increased as well. Such a microporosity was not present in the OCP coating. Nevertheless, OCP coating surface was rough as well, due to large crystals that perpendicularly grew on the implant surface.

The above-mentioned material characteristics: chemical composition, microporosity, crystallinity and surface roughness are all of great importance for osteoinductive potential of a material.

As shown in Table III, the presence of OCP coating increased the osteoinductive potential of all biomaterials. Uncoated Ti6Al4V and HA, that did not show ectopic bone formation in this study, did induce ectopic bone formation when coated with OCP. The amount of bone induced by uncoated BCP increased after the application of the OCP coating on its surface. The fact that uncoated BCP did and uncoated HA did not show any bone induction is caused by differences in their chemistry and structure as earlier described by Yuan *et al*. [12]. The reason for the poor osteoinductive performance of the coated polymer might be explained by the fact that this implant was very soft and unable to maintain its porous shape after implantation. Continuous movement of the muscle caused too much pressure on the PEGT–PBT implant, making the implant flat and its pores closed.

Although we are continuously getting more insight into the importance of many different materials characteristics (chemistry, composition, macro- and microstructure) on osteoinductive behaviour of biomaterials [10–12, 28], the exact mechanism of osteoinduction remains unknown. Concerning this mechanism, we hypothesise: (1) osteoinductive materials exert a direct effect on the growth and differentiation of relevant cells that attach to them and (2) the surface of osteoinductive materials helps collecting relevant proteins, which in their turn exert an osteoinductive effect on the recruited cells.

In both cases, the presence of porosity plays an important role. Nutrients can easily be supplied through the interconnected porous structure. On the other hand, pore walls can provide a protected area, without a strong fluid movement, giving the cells space to differentiate towards osteogenic lineage. The presence of certain CaP phase with certain microstructure leads to a dissolution process, and therewith release of calcium and phosphate ions. This process results in a CaP supersaturation at the vicinity of the implant surface, eventually causing precipitation of bone like carbonated apatite layer, possibly accompanied with coprecipitation of relevant proteins from body fluids. This process, together with the presence of protected areas in the pores, sufficient nutrients supply and a rough surface that is responsible for a good cell attachment, might all lead to the start of extraskeletal bone formation.

This study shows that we are able to produce an OCP coating on various kinds of porous implants by following a biomimetic route. OCP coating can improve the osteoinductive potential of various materials. Previous studies [29] showed that osteoinductive materials are also performing better in orthotopic sites than the non-inductive ones suggesting the importance of osteoinductivity for the clinics. The combination of the advantages of biomimetic coating method above traditional methods, and a good osteoinductivity of OCP coating that can be produced by using method, opens new possibilities for designing more advanced orthopaedic implants.

Acknowledgment

A part of this study was financially supported by the EU ''Intelliscaf'' Project (G5RD-CT-2002-00697).

References

1. H. YAMASAKI, *Jpn. J. Oral. Biol.* **32** (1990) 190.
2. X. ZHANG, in ''Bioceramics and Human Body'' (Elsevier Science, Amsterdam, 1991) p. 408.
3. C. P. A. T. KLEIN, K. DE GROOT, W. CHEN, Y. LI and X. ZHANG, *Biomaterials* **15** (1994) 31.
4. H. YAMASAKI and H. SAKI, *ibid.* **13** (1992) 308.
5. U. RIPAMONTI, *ibid.* **17** (1996) 31.
6. U. RIPAMONTI, *J. Bone Joint. Surg.* **73A** (1991) 692.
7. K. VARGERVIK, in ''Bone Grafts and Bone Substitutes'' (W.B. Saunders, Philadelphia 1992) p. 112.
8. H. YUAN, Z. YANG, P. ZOU, Y. LI and X. ZHANG, *Biomed. Eng. Appli. Bas. Com.* **9** (1997) 697.
9. H. YUAN, J. D. DE BRUIJN, Z. YANG, Y. LI, K. DE GROOT and X. ZHANG, *J. Mater. Sci. Mater. Med.* **9** (1998) 723.
10. H. YUAN, K. KURASHINA, J. D. DE BRUIJN, Y. LI, K. DE GROOT and X. ZHANG, *Biomaterials* **20** (1999) 1799.
11. H. YUAN, J. D. DE BRUIJN, Y. LI, J. FENG, K. DE GROOT and X. ZHANG, *J. Mater. Sci. Mater. Med.* **12** (2001) 7.
12. H. YUAN, M. VAN DEN DOEL, S. LI, C. A. VAN BLITTERSWIJK, K. DE GROOT and J. D. DE BRUIJN, *ibid.* **13** (2002) 1271.
13. J. M. TOTH, K. L. LYNCH and D. A. HACKBARTH, *Bioceramics* **6** (1993) 9.
14. H. YUAN, Y. LI, K. KURASHINA and X. ZHANG, in ''Biomedical Research in the Far East (III)'' (Kyoto 1997) 1531.
15. H. YUAN, J. D. DE BRUIJN, R. DALMEIJER, P. LAYROLLE, C. A. VAN BLITTERSWIJK, X. ZHANG and K. DE GROOT, in ''Osteoinduction by Calcium Phosphates'' (CIP Data Koninkelijke Bibliotheek, The Hague 2001) p. 123.
16. F. BARRERE, C. M. VAN DER VALK, R. A. J. DALMEIJER, G. MEIJER, C. A. VAN BLITTERSWIJK, K. DE GROOT and P. LAYROLLE, *J. Biomed. Mater. Res.* **66A** (2003) 779.

17. L. I. HAVELIN, L. B. ENGESAETER, O. FURNES, S. A. LIE and S. E. VOLLSET, *Acta Orthop. Scand.* **71** (2000) 337.
18. P. DUCHEYNE, W. VAN RAEMDONCK, J. C. HEUGHEBAERT and M. HEUGHEBAERT, *Biomaterials* **7** (1986) 97.
19. J. L. ONG, L. C. LUCAS, W. R. LACEFIELD and E. D. RIGNEY, *ibid.* **13** (1992) 249.
20. B. BEN-NISSAN, C. S. CHAI and K. A. GROSS, *Bioceramics* **10** (1997) 175.
21. T. KOKUBO, H. KUSHITANI, S. SAKKA, T. KITSUGI and T. YAMAMURO, *J. Biomed. Mater. Res.* **24** (1990) 721.
22. F. BARRERE, P. LAYROLLE, C. A. VAN BLITTERSWIJK and K. DE GROOT, *J. Mat. Sci. Mat. Med.* **12** (2001) 529.
23. P. HABIBOVIC, F. BARRERE, C. A. VAN BLITTERSWIJK, K. DE GROOT and P. LAYROLLE, *J. Am. Ceram. Soc.* **85** (2002) 517.
24. J. P. LI, S. H. LI, K. DE GROOT and P. LAYROLLE, *Key Eng. Mater.* **51** (2002) 218.
25. C. DU, P. KLASENS, R. E. HAAN, J. BEZEMER, F. Z. CUI, K. DE GROOT and P. LAYROLLE, *J. Biomed. Mater. Res.* **59** (2002) 535.
26. H. YUAN, J. D. DE BRUIJN, X. ZHANG, C. A. VAN BLITTERSWIJK and K. DE GROOT, in Proceedings of the 16th European Conference on Biomaterials, London, UK, September 2001, p. 209.
27. S. FUJIBAYASHI, M. NEO, H. M. KIM, T. KOKUBO and T. NAKAMURA, *Biomaterials* in press.
28. A. MAGAN and U. RIPAMONTI, *J. Craniofac. Surg.* **7** (1996) 71.
29. H. YUAN, J. D. DE BRUIJN, C. A. VAN BLITTERSWIJK and K. DE GROOT, in Proceedings of the 17th European Conference on Biomaterials, Barcelona, Spain, October 2002, p. 156.

Received 4 October
and accepted 10 October 2003